

Activationless charge transport across 4.5 to 22 nm in molecular electronic junctions

Haijun Yan^a, Adam Johan Bergren^a, Richard McCreery^{a,b,1}, Maria Luisa Della Rocca^c, Pascal Martin^d, Philippe Lafarge^c, and Jean Christophe Lacroix^d

^aNational Institute for Nanotechnology, Edmonton, AB, Canada T6G 2M9; ^bDepartment of Chemistry, University of Alberta, Edmonton, AB, Canada T6G 2G2; ^cLaboratoire Matériaux et Phénomènes Quantiques (MPQ), Unité Mixte de Recherche 7162, Centre National de la Recherche Scientifique (CNRS), Université Paris Diderot, Sorbonne Paris Cité, 75205 Paris Cedex 13, France; and ^dLaboratoire Interfaces, Traitements, Organisation et Dynamique des Systèmes (ITODYS), Unité Mixte de Recherche 7086, Centre National de la Recherche Scientifique (CNRS), Université Paris Diderot, Sorbonne Paris Cité, 75205 Paris Cedex 13, France

Edited by Mark A. Ratner, Northwestern University, Evanston, IL, and approved February 20, 2013 (received for review December 14, 2012)

In this work, we bridge the gap between short-range tunneling in molecular junctions and activated hopping in bulk organic films, and greatly extend the distance range of charge transport in molecular electronic devices. Three distinct transport mechanisms were observed for 4.5–22-nm-thick oligo(thiophene) layers between carbon contacts, with tunneling operative when $d < 8$ nm, activated hopping when $d > 16$ nm for high temperatures and low bias, and a third mechanism consistent with field-induced ionization of highest occupied molecular orbitals or interface states to generate charge carriers when $d = 8–22$ nm. Transport in the 8–22-nm range is weakly temperature dependent, with a field-dependent activation barrier that becomes negligible at moderate bias. We thus report here a unique, activationless transport mechanism, operative over 8–22-nm distances without involving hopping, which severely limits carrier mobility and device lifetime in organic semiconductors. Charge transport in molecular electronic junctions can thus be effective for transport distances significantly greater than the 1–5 nm associated with quantum-mechanical tunneling.

all-carbon molecular junction | attenuation coefficient | field ionization | strong electronic coupling

Charge transport mechanisms in organic and molecular electronics underlie the ultimate functionality of a new generation of electronic devices. Understanding, controlling, and designing molecular devices for use as practical components requires an intimate knowledge of the system energy levels and operative transport mechanisms, and how key variables such as molecule length, identity, temperature, etc., affect device performance parameters. Especially interesting in this context is the relationship between organic electronic devices, which typically have active layer thicknesses of tens to hundreds of nanometers, and molecular electronic devices reported to date, in which at least one dimension for charge propagation is below 10 nm. Indeed, many types of functional organic electronic devices have been demonstrated, including thin-film transistors, organic light-emitting diodes, and memory cells (1, 2). Bridging the gap between organic and molecular devices may therefore reveal pathways for improving the performance of such devices, or even lead to new types of devices based on alternative transport mechanisms.

The great majority of molecular electronic devices investigated to date have transport distances of < 5 nm between the contacts, where the prevalent transport mechanism is quantum-mechanical tunneling. For this distance range, there is general agreement that the conductance scales exponentially with length, with an attenuation coefficient (β), defined as the slope of $\ln J$ vs. thickness (d), equal to 8 to 9 nm⁻¹ for aliphatic molecules (3–6) and 2–3 nm⁻¹ for aromatic molecules (7–14). A few molecular electronic systems have been investigated beyond 5 nm (15, 16), some of which exhibit a decrease in β to less than 1 nm⁻¹. Such small values of β are significant both practically (17, 18) and fundamentally (19–22), because they imply transport across distances much greater than the dimensions of single molecules and may enable complex

molecular circuits. These low β -values are often dependent on temperature and have been attributed to activated hopping by a redox exchange mechanism (10, 23). However, phase-coherent tunneling has also been proposed for cases where the molecules have orbitals close in energy to the contact Fermi level (15, 24), resulting in minimal temperature dependence.

In this paper, we investigate the frontier between molecular and organic electronics by describing the electrical characteristics of conjugated molecular junctions of the structure carbon/molecule/carbon/Au over a wide range of thickness (from 4.5 to 22 nm). Reduction of a diazonium reagent of bis-thienylbenzene (BTB) (25–29) on carbon surfaces permits formation of molecular films of controlled thickness consisting of conjugated oligomers, and the electronic junction is completed by electron-beam deposition of carbon and gold (30). Such grafted oligo(BTB) layers can be easily *p*-doped and switched from insulating to conductive states in electrochemical conditions (25–28). Previous transport measurements in planar Au junctions containing a 7-nm-thick BTB molecular layer were explained with a mixed-transport mechanism combining a conducting molecular region with a tunnel barrier (31). In the present work, temperature and electrical field dependence of transport were analyzed to determine the likely transport mechanisms in three thickness regions: less than 8 nm, 8–16 nm, and greater than 16 nm. The results indicate three distinct transport mechanisms: coherent tunneling for $d < 8$ nm, activated hopping similar to that observed in bulk organic semiconductors for $d > 16$ nm, and a third mechanism which occurs over a broad range of temperature and electric field for molecular layer thicknesses of 8–22 nm.

Results and Discussion

Molecular junctions (area = 0.0013 cm²) were constructed (9, 30, 32, 33) on pyrolyzed photoresist film (PPF), which is a flat, conducting sp² hybridized carbon surface described in detail previously (34). *SI Appendix, Fig. S1* shows a junction schematic and the four-wire electronic apparatus used for device characterization; *SI Appendix, sections 2 and 3* detail the fabrication procedure and thickness determination. Current density vs. voltage (JV) curves obtained for PPF/BTB/e-C/Au junctions with BTB thickness from 4.5 to 22 nm are shown in Fig. 1*A* and *C* for linear and semilog J scales, respectively. Fig. 1*B* and *D* shows a selection of the same devices collected at temperature (T) < 10 K on linear (Fig. 1*B*) and semilog (Fig. 1*D*) scales. It is clear from analysis of these curves that: (i) J is nonlinear in V , but nearly symmetric with

Author contributions: R.M. and J.C.L. designed research; H.Y. and A.J.B. performed research; P.M. contributed new reagents/analytic tools; H.Y., A.J.B., R.M., M.L.D.R., P.L., and J.C.L. analyzed data; and H.Y., A.J.B., R.M., and J.C.L. wrote the paper.

The authors declare no conflict of interest.

This article is a PNAS Direct Submission.

¹To whom correspondence should be addressed. E-mail: richard.mccreery@ualberta.ca.

This article contains supporting information online at www.pnas.org/lookup/suppl/doi:10.1073/pnas.1221643110/-DCSupplemental.

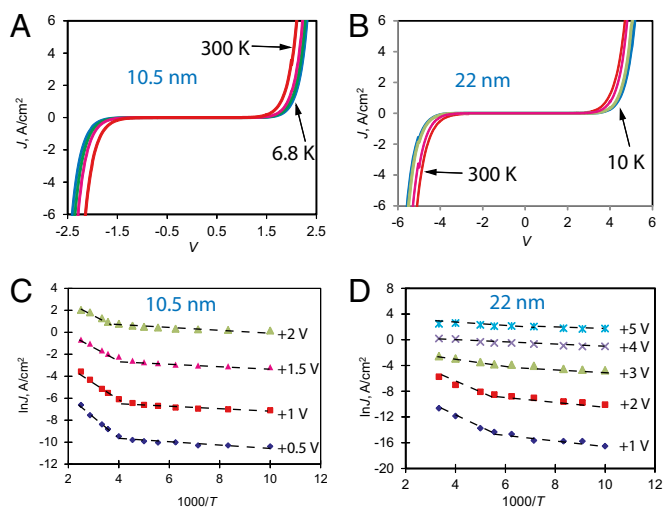


Fig. 3. JV curves at <10, 100, 200, and 300 K for (A) 10.5- and (B) 22-nm junctions. Arrhenius plots of $\ln J$ vs. $1000/T$ for (C) 10.5- and (D) 22.2-nm BTB junctions, obtained at the indicated bias values. Linear portions are identified by dashed lines, and a complete listing of E_a appears in Table 1. *SI Appendix, Fig. S8A* shows the dependence of E_a on bias.

origin of such behavior, an important and exciting consequence is the possibility of long distance, activationless charge transport across distances not possible with coherent tunneling.

Several classical mechanisms possible in molecular junctions in addition to tunneling and hopping include thermionic (i.e., Schottky) emission, field ionization (i.e., Fowler–Nordheim, or FN, tunneling), Poole–Frenkel (PF) transport between Coulombic traps, and variable range hopping (VRH). Of these, FN tunneling is independent of temperature, and is predicted to yield a linear plot of $\ln(J/E^2)$ vs. $1/E$ (i.e., an FN plot), where E is the electric field (41, 42). Fig. 4A shows an overlay of FN plots of BTB

Table 1. Arrhenius slopes for varying thickness and bias

d , nm	V	E_a , meV		
		5–50 K	100–200 K	200–300 K
4.5	0.1	0.16	9	30
	0.2	0.12	6	24
	0.5	0.1		
8.0	0.2	0.28	5	26
	0.5	0.12	4	39
	1.0	0.04	4	48
	1.5	0.08	3	43
10.5	0.2	0.15	13	85
	0.5	0.43	8	79
	1.0	0.01	8	75
	1.5	0.1	8	54
16	2.0	0.08	6	36
	0.2			291
	0.5		10	209
	1.0		5	175
	1.5		2	130
22	2.0		2	99
	3.0		1	60
	1.0	0.26	43	160
	2.0	0.43	33	119
	3.0	0.34	22	47
	4.0	0.09	13	28
	5.0	0.03	10	9

junctions as a function of BTB thickness at 300 K. Note that the curves for $d = 8.0, 10.5,$ and 22 nm converge at high field, implying that transport is controlled by electric field above $E = 1$ MV/cm. Fig. 4B shows the same plot for the 8.0- and 22-nm thicknesses at 6 and 300 K. It is clear that the curves converge at high E for both temperatures, but do not exhibit the linear region predicted from FN theory. VRH is characterized by a linear plot of $\ln J$ vs. $T^{-1/4}$ for three-dimensional Mott VRH or $\ln J$ vs. or $T^{-1/2}$ for one-dimensional Mott VRH or Efros–Shklovskii VRH (43–45). Several such plots are shown in *SI Appendix, Fig. S7*, and exhibit no linear regions for the temperature dependence shown in Fig. 3. We conclude that neither VRH nor FN mechanisms are consistent with the JV results over the entire temperature and bias ranges examined. PF and Schottky mechanisms predict linearity of $\ln(J/E)$ vs. $E^{1/2}$, and such plots are shown in Fig. 4C at 300 K and Fig. 4D for <10 K. The curves for $d = 8.0$ – 22 nm converge at high E at both temperatures, and the low- T case shows excellent linearity of $\ln(J/E)$ vs. $E^{1/2}$, especially for $d = 22$ nm for which $R^2 = 0.9989$ over 8 orders of magnitude of J/E . Both mechanisms also predict linearity of E_a vs. $E^{1/2}$ with intercepts at zero field equal to the barrier height. Such plots are shown in *SI Appendix, Fig. S8A*, exhibiting reasonable linearity for 16- and 22-nm junctions for the 200- to 300-K Arrhenius slopes, and intercepts at zero field indicating barrier heights of ~ 350 meV (16 nm) and ~ 300 meV (22 nm). These results indicate that PF or Schottky mechanisms may be valid above 200 K for $d \geq 16$ nm, where a voltage-dependent E_a is observed (Table 1). PF transport has been proposed for organic semiconductors across distances greater than studied here, and is consistent with observed E dependence (46–49).

However, PF and Schottky mechanisms are not consistent with the weak temperature dependence below 200 K. Comparing Fig. 4C and D, the experimental curves are very similar for 300 K and <10 K, contrary to the predictions of Schottky and PF equations for ~ 300 -meV barriers. As shown in *SI Appendix, Fig. S8B*, the slope of the experimental $\ln(J/E)$ vs. $E^{1/2}$ plot increases by a factor of 1.32 between 300 and 6 K for $d = 22$ nm, although theory predicts it should increase by a factor of >50 ($300/6$) for either PF or Schottky mechanisms. We conclude that classical Schottky or PF transport cannot explain transport in BTB junctions, nor can the FN or VRH models discussed above. Therefore, there must be another mechanism operative below 200 K which becomes dominant at

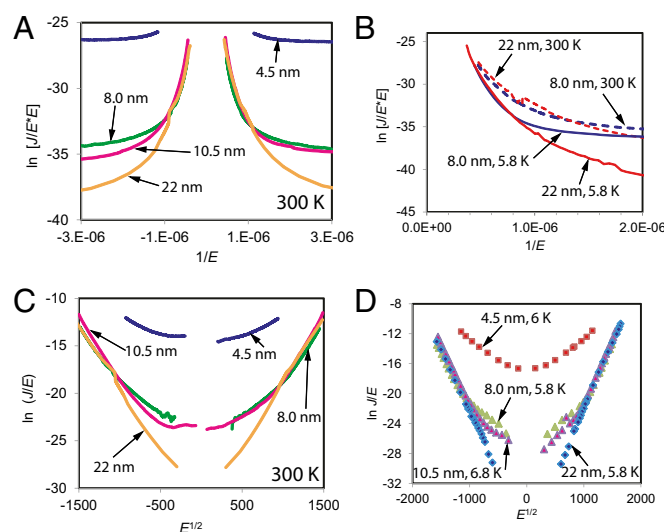


Fig. 4. (A) FN plot of $\ln(J/E^2)$ vs. $1/E$, where E = electric field (V/cm) at 300 K for the indicated BTB thicknesses. (B) FN plot for 8.0- and 22-nm BTB devices at <5.8 and 300 K. (C and D) PF plots of $\ln(J/E)$ vs. $E^{1/2}$ for the same four BTB thicknesses at (C) 300 and (D) <10 K.

moderate and high electric field. This mechanism has not been reported previously for molecular junctions, and is temperature independent with a β of $\sim 1.0 \text{ nm}^{-1}$ for BTB junctions with $d = 8\text{--}22 \text{ nm}$, as shown in Fig. 2.

Given that classical mechanisms are not consistent with the BTB JV behavior, we note a few recent observations of field-driven mechanisms for transport in much thicker organic films ($>100 \text{ nm}$) (46–49). Whereas transport dimensions and bias voltages were much larger than the 4.5–22-nm range studied here, a linear dependence of $\ln J$ vs. $E^{1/2}$ was observed, as was T -independent conductance at low T . Although the mechanism is controversial, these observations were attributed to field-assisted hopping (46, 48), field-assisted tunneling (47, 48), multistep tunneling (47), or behavior similar to a Luttinger liquid (49). For the case of polythiophene thin-film transistors, a transition from PF-like behavior at room temperature to temperature-independent field-emission hopping with an $E^{1/2}$ dependence at low temperature was reported (48).

In the present case, to explain transport in the region where $\beta \sim 1.0 \text{ nm}^{-1}$, we propose that field ionization occurs when the stabilization energy of an electron in the applied field exceeds the trap depth, similar to PF transport. The “trap” could be a localized state such as the highest occupied molecular orbital (HOMO) of oligo (BTB) or a hybrid orbital that has density on both the molecule and the contact, such as a “gap state” (50). Such hybrid states are likely in a system with a covalently bonded molecular layer, which is known to induce Fermi-level pinning and strong electronic coupling (14, 50). The distinction between classical PF behavior and the proposed field ionization mechanism lies in the events following ionization. Conventional activated PF transport involves thermal carrier generation assisted by the applied field, and subsequent transport characterized by the mobility of the carriers. The very short transport distances in the BTB junctions may permit ballistic carrier transport following ionization, such that ionization and transport are concerted. Rapid refilling of the field-ionized orbital from one electrode would permit further ionization and current flow with no need for reorganization, thus maintaining activationless transport. An additional possibility after the initial field-ionization event is relaxation of the ionized centers to form polarons, resulting in new conduction channels with high conductivity. Such polarons are expected to be 5–10 nm long, and are

therefore comparable to the thickness of several of the BTB junctions studied, so that a single intrachain transfer is sufficient for charge transport within the molecular layer (51, 52). Such intrachain transport is expected to have activation energies in the 40–80-meV range (51), consistent with some of the low observed E_a values.

Conclusions

Charge transport in 4.5–22-nm BTB molecular junctions is characterized by three attenuation factors and three distinct mechanisms. For $d < 8 \text{ nm}$, current is controlled by coherent tunneling, with minimal temperature dependence and $\beta = 3 \text{ nm}^{-1}$, as described previously for conjugated molecular junctions (9, 14, 30). For low field and high T , the thickest devices ($d > 16 \text{ nm}$) exhibit hopping transport with $\beta < 0.1 \text{ nm}^{-1}$ and strong T dependence, similar to that observed for bulk organic semiconductors. For a wide range of thickness (8–22 nm) and T (6–300 K), a third, nearly activationless mechanism with $\beta \sim 1 \text{ nm}^{-1}$ and E_a between 0 and 80 meV is observed, for which the current is controlled mainly by the electric field. This mechanism is consistent with field-induced ionization of molecular HOMOs or interface states to generate charge carriers. The field required for onset of ionization is presumably dependent on the energy of the orbital to be ionized relative to the system Fermi level. Following ionization, the empty state may be rapidly refilled from the negatively biased electrode, or may reorganize to form a polaron and a new conducting channel. Activated hopping is important for thicker films at high T and low electric field, whereas field ionization becomes dominant at high electric field and all temperatures examined. In addition to identifying an additional transport mechanism for molecular junctions, the current report unifies the fields of molecular and organic electronics by covering distances from short-range tunneling to activated, long-range hopping which underlies transport in bulk organic semiconductors.

ACKNOWLEDGMENTS. The authors thank Peng Li (National Institute for Nanotechnology electron microscopy facility) for preparation and microscopy of the junction cross-section and acknowledge financial support from the National Research Council (Canada), the Natural Science and Engineering Research Council (Canada), the University of Alberta, Alberta Innovates Technology Futures, the Agence Nationale Recherche (France), and the Centre National de la Recherche Scientifique (France).

- Naber WJM, Faez AS, van der Wiel AWG (2007) Organic spintronics. *J Phys D Appl Phys* 40(12):R205–R228.
- Scott JC, Bozano LD (2007) Nonvolatile memory elements based on organic materials. *Adv Mater (Deerfield Beach Fla)* 19(11):1452–1463.
- Akkerman HB, De Boer B (2008) Electrical conduction through single molecules and self-assembled monolayers. *J Phys Condens Matter* 20:013001.
- Bonifas AP, McCreery RL (2010) ‘Soft’ Au, Pt and Cu contacts for molecular junctions through surface-diffusion-mediated deposition. *Nat Nanotechnol* 5(8):612–617.
- Bonifas AP, McCreery RL (2011) Assembling molecular electronic junctions one molecule at a time. *Nano Lett* 11(11):4725–4729.
- Weiss EA, et al. (2007) Influence of defects on the electrical characteristics of mercury-drop junctions: Self-assembled monolayers of n-alkanethiolates on rough and smooth silver. *J Am Chem Soc* 129(14):4336–4349.
- Kronemeijer AJ, et al. (2010) Electrical characteristics of conjugated self-assembled monolayers in large-area molecular junctions. *Appl Phys Lett* 97(17):173302.
- Anariba F, Steach JK, McCreery RL (2005) Strong effects of molecular structure on electron transport in carbon/molecule/copper electronic junctions. *J Phys Chem B* 109(22):11163–11172.
- Bergren AJ, McCreery RL, Stoyanov SR, Gusarov S, Kovalenko A (2010) Electronic characteristics and charge transport mechanisms for large area aromatic molecular junctions. *J Phys Chem C* 114(37):15806–15815.
- Ho Choi S, Kim B, Frisbie CD (2008) Electrical resistance of long conjugated molecular wires. *Science* 320(5882):1482–1486.
- Engelkes VB, Beebe JM, Frisbie CD (2004) Length-dependent transport in molecular junctions based on SAMs of alkanethiols and alkanedithiols: Effect of metal work function and applied bias on tunneling efficiency and contact resistance. *J Am Chem Soc* 126(43):14287–14296.
- Liu H, et al. (2008) Length-dependent conductance of molecular wires and contact resistance in metal-molecule-metal junctions. *ChemPhysChem* 9(10):1416–1424.
- Salomon A, et al. (2003) Comparison of electronic transport measurements on organic molecules. *Adv Mater (Deerfield Beach Fla)* 15(22):1881–1890.
- Sayed SY, Fereiro JA, Yan H, McCreery RL, Bergren AJ (2012) Charge transport in molecular electronic junctions: Compression of the molecular tunnel barrier in the strong coupling regime. *Proc Natl Acad Sci USA* 109(29):11498–11503.
- Sedghi G, et al. (2012) Comparison of the conductance of three types of porphyrin-based molecular wires: β , meso, β -fused tapes, meso-Butadiyne-linked and twisted meso-meso linked oligomers. *Adv Mater (Deerfield Beach Fla)* 24(5):653–657.
- Tuccitto N, et al. (2009) Highly conductive approximately 40-nm-long molecular wires assembled by stepwise incorporation of metal centres. *Nat Mater* 8(1):41–46.
- DiBenedetto SA, Facchetti A, Ratner MA, Marks TJ (2009) Charge conduction and breakdown mechanisms in self-assembled nanodielectrics. *J Am Chem Soc* 131(20):7158–7168.
- Goldsmith RH, et al. (2008) Unexpectedly similar charge transfer rates through benzoannulated bicyclo[2.2.2]octanes. *J Am Chem Soc* 130(24):7659–7669.
- Berlin YA, Grozema FC, Siebbeles LDA, Ratner MA (2008) Charge transfer in donor-bridge-acceptor systems: Static disorder, dynamic fluctuations, and complex kinetics. *J Phys Chem C* 112(29):10988–11000.
- Lindsay SM, Ratner MA (2007) Molecular transport junctions: Clearing mists. *Adv Mater (Deerfield Beach Fla)* 19(1):23–31.
- Mujica V, Kemp M, Ratner MA (1994) Electron conduction in molecular wires. I. A scattering formalism. *J Chem Phys* 101(8):6849–6855.
- Mujica V, Kemp M, Ratner MA (1994) Electron conduction in molecular wires. II. Application to scanning tunneling microscopy. *J Chem Phys* 101(8):6856–6864.
- Choi SH, et al. (2010) Transition from tunneling to hopping transport in long, conjugated oligo-imine wires connected to metals. *J Am Chem Soc* 132(12):4358–4368.
- Sedghi G, et al. (2011) Long-range electron tunnelling in oligo-porphyrin molecular wires. *Nat Nanotechnol* 6(8):517–523.
- Fave C, et al. (2007) Tunable electrochemical switches based on ultrathin organic films. *J Am Chem Soc* 129(7):1890–1891.
- Fave C, et al. (2008) Electrochemical switches based on ultrathin organic films: From diode-like behavior to charge transfer transparency. *J Phys Chem C* 112(47):18638–18643.
- Santos L, Ghilane J, Lacroix JC (2012) Formation of mixed organic layers by stepwise electrochemical reduction of diazonium compounds. *J Am Chem Soc* 134(12):5476–5479.

28. Santos L, et al. (2010) Host-guest complexation: A convenient route for the electroreduction of diazonium salts in aqueous media and the formation of composite materials. *J Am Chem Soc* 132(5):1690–1698.
29. Stockhausen V, et al. (2009) Grafting oligothiophenes on surfaces by diazonium electroreduction: A step toward ultrathin junction with well-defined metal/oligomer interface. *J Am Chem Soc* 131(41):14920–14927.
30. Yan H, Bergren AJ, McCreery RL (2011) All-carbon molecular tunnel junctions. *J Am Chem Soc* 133(47):19168–19177.
31. Martin P, Della Rocca ML, Anthore A, Lafarge P, Lacroix J-C (2012) Organic electrodes based on grafted oligothiophene units in ultrathin, large-area molecular junctions. *J Am Chem Soc* 134(1):154–157.
32. Bergren AJ, Harris KD, Deng F, McCreery RL (2008) Molecular electronics using diazonium-derived adlayers on carbon with Cu top contacts: Critical analysis of metal oxides and filaments. *J Phys Condens Matter* 20(37):374117.
33. Mahmoud AM, Bergren AJ, Pekas N, McCreery RL (2011) Towards integrated molecular electronic devices: Characterization of molecular layer integrity during fabrication processes. *Adv Funct Mater* 21(12):2273–2281.
34. Ranganathan S, McCreery RL, Majji SM, Madou M (2000) Photoresist-derived carbon for microelectrochemical applications. *J Electrochem Soc* 147(1):277–282.
35. Hines T, et al. (2010) Transition from tunneling to hopping in single molecular junctions by measuring length and temperature dependence. *J Am Chem Soc* 132(33):11658–11664.
36. Lee SK, et al. (2012) Universal temperature crossover behavior of electrical conductance in a single oligothiophene molecular wire. *ACS Nano* 6(6):5078–5082.
37. Goh C, Kline RJ, McGehee MD, Kadnikova EN, Frechet JMJ (2005) Molecular-weight-dependent mobilities in regioregular poly(3-hexyl-thiophene) diodes. *Appl Phys Lett* 86(12):122110–122113.
38. Nolasco JC, et al. (2010) Extraction of poly(3-hexylthiophene) (P3HT) properties from dark current voltage characteristics in a P3HT/n-crystalline-silicon solar cell. *J Appl Phys* 107(4):044505.
39. Jiang X, et al. (2001) Mobilities of charge carriers hopping between [small pi]-conjugated polymer chains. *J Mater Chem* 11(12):3043–3048.
40. Cornil J, Beljonne D, Calbert JP, Brédas JL (2001) Interchain interactions in organic π -conjugated materials: Impact on electronic structure, optical response, and charge transport. *Adv Mater (Deerfield Beach Fla)* 13(14):1053–1067.
41. Aswal DK, Lenfant S, Guerin D, Yakhmi JV, Vuillaume D (2005) Fowler-Nordheim tunnelling and electrically stressed breakdown of 3-mercaptopropyltrimethoxysilane self-assembled monolayers. *Nanotechnology* 16(12):3064–3068.
42. Sze SM, ed (1981) *Physics of Semiconductor Devices*, 2nd Ed (Wiley, New York).
43. Hill RM (1976) Variable-range hopping. *Phys Status Solidi* 34:601–613.
44. Jang EY, et al. (2012) Fibers of reduced graphene oxide nanoribbons. *Nanotechnology* 23(23):235601.
45. Mott NF, Davis EA (1979) *Electronic Processes in Non-Crystalline Materials* (Clarendon, Oxford).
46. Prigodin VN, Epstein AJ (2007) Comment on “Voltage-induced metal-insulator transition in polythiophene field-effect transistors.” *Phys Rev Lett* 98(25):259703.
47. Wei JH, Gao YL, Wang XR (2009) Inverse square-root field dependence of conductivity in organic field-effect transistors. *Appl Phys Lett* 94(7):073301.
48. Worne JH, Anthony JE, Natelson D (2010) Transport in organic semiconductors in large electric fields: From thermal activation to field emission. *Appl Phys Lett* 96(5):53308.
49. Yuen JD, et al. (2009) Nonlinear transport in semiconducting polymers at high carrier densities. *Nat Mater* 8(7):572–575.
50. Braun S, Salaneck WR, Fahlman M (2009) Energy-level alignment at organic/metal and organic/organic interfaces. *Adv Mater (Deerfield Beach Fla)* 21(14–15):1450–1472.
51. Lacroix JC, Chane-Ching KI, Maquère F, Maurel F (2006) Intrachain electron transfer in conducting oligomers and polymers: The mixed valence approach. *J Am Chem Soc* 128(22):7264–7276.
52. Geskin VM, Dkhissi A, Brédas JL (2003) Oligothiophene radical cations: Polaron structure in hybrid DFT and MP2 calculations. *Int J Quantum Chem* 91(3):350–354.